Mon. Not. R. Astron. Soc. **000**, 000–000 (0000) Printed 6 August 2014 (MN LATEX style file v2.2)

Galaxy Zoo: Evidence for Diverse Star Formation Histories through the Green Valley

R. J. Smethurst,[1] C. J. Lintott,[1,2] B. D. Simmons,[1] K. Schawinski,[3] K. L. Masters,[4] K. W. Willett,[5] P. J. Marshall,[6,1] S. Bamford,[7] T. Melvin,[4] R. A. Skibba [8]

[1] *Oxford Astrophysics, Department of Physics, University of Oxford, Denys Wilkinson Building, Keble Road, Oxford, OX1 3RH, UK*
[2] *Adler Planetarium, 1300 S Lake Shore Drive, Chicago, IL, 60605, USA*
[3] *Institute for Astronomy, Department of Physics, ETH Zurich, Wolfgang-Pauli Strasse 27, CH-8093 Zurich, Switzerland*
[4] *Institute of Cosmology and Gravitation, University of Portsmouth, Dennis Sciama Building, Barnaby Road, Portsmouth, PO1 3FX, UK*
[5] *School of Physics and Astronomy, University of Minnesota, 116 Church St SE, Minneapolis, MN 55455, USA*
[6] *Kavli Institute for Particle Astrophysics and Cosmology, Stanford University, 452 Lomita Mall, Stanford, CA 95616, USA*
[7] *School of Physics and Astronomy, The University of Nottingham, University Park, Nottingham, NG7 2RD, UK*
[8] *Center for Astrophysics and Space Sciences, University of California San Diego, 9500 Gilman Drive, La Jolla, CA 92093, USA*

6 August 2014

ABSTRACT

Does galactic evolution proceed through the green valley via multiple pathways or as a single population? Motivated by recent results highlighting radically different evolutionary pathways between early- and late-type galaxies, we present results from a simple Bayesian approach to this problem wherein we model the star formation history of a galaxy and compare the predicted and observed optical and near-ultraviolet colours. We use a novel method to investigate the morphological differences between the most probable values for these parameters for both disc-like and elliptical-like populations of galaxies, by using probabilistic estimates of morphology from Galaxy Zoo⋆. We find that the parameters for the green valley galaxies for both major morphologies follow those of the red sequence but at later times, predicting the build up of the red sequence. The green valley is therefore a transitional population, regardless of morphology, however the rate of this transition depends on the morphology.

1 INTRODUCTION

Previous large scale surveys of galaxies have revealed a bimodality in the colour-magnitude diagram (CMD) with two distinct populations; one at relatively low mass, with blue optical colours and another at relatively high mass, with red optical colours (Baldry et al. 2004, 2006; Willmer et al. 2006; Ball, Loveday & Brunner 2008; Brammer et al. 2009). These populations were dubbed the 'blue cloud' and 'red sequence' respectively. The Galaxy Zoo project (Lintott et al. 2011), which incorporated morphological classifications for a million galaxies revealed that this bimodality is not entirely morphology driven (Bamford et al. 2009; Skibba et al. 2009), detecting spiral galaxies in the red sequence (Masters et al. 2010a) and elliptical galaxies in the blue cloud (Schawinski et al. 2009).

The sparsely populated colour space between these two populations, the so-called 'green valley', provides clues to the nature and duration of galaxies' transitions from blue to red. This transition must therefore occur on rapid timescales, otherwise we would find an accumulation of galaxies residing in the green valley, rather than an accumulation in the red sequence as is observed (Arnouts et al. 2007; Martin et al. 2007). Green valley galaxies have therefore long been thought of as the 'crossroads' of galaxy evolution; a transition population between the two main galactic stages of the star forming blue cloud and the 'dead' red sequence (Bell et al. 2004; Wyder et al. 2007; Schiminovich et al. 2007; Martin et al. 2007; Faber et al. 2007; Mendez et al. 2011; Gonçalves et al. 2012; Schawinski et al. 2014).

The intermediate colours of these green valley galaxies have been interpreted as evidence for recent quenching (suppression) of star formation (Salim et al. 2007). Star forming galaxies are observed to lie on a well defined mass-SFR relation, however quenching a galaxy causes it to depart from this relation (Noeske et al. 2007; Peng et al. 2010; see Figure 5)

By studying the galaxies which have just left this mass-SFR relation, we can probe the quenching mechanisms by which this occurs. There have been many previous theories for the initial triggers of these quenching mechanisms, including negative feedback from AGN (Schawinski et al. 2007), mergers (Darg et al. 2010), supernovae winds

⋆ This investigation has been made possible by the participation of more than 250,000 users in the Galaxy Zoo project. Their contributions are individually acknowledged at http://www.galaxyzoo.org/volunteers.aspx

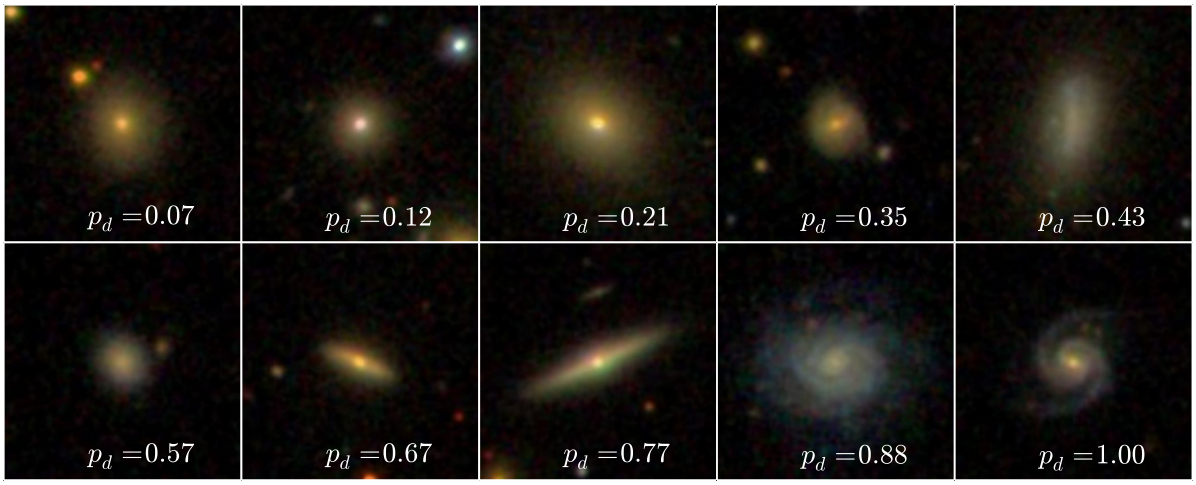

Figure 1. Mosaic of SDSS images showing the continuous probabilistic nature of the Galaxy Zoo sample. The debiased disc vote fraction (see Willett et al. 2013) for each galaxy is shown.

(Marasco, Fraternali & Binney 2012) and secular evolution (Masters et al. 2010a, 2011). By investigating the *amount* of quenching that has occurred between the blue cloud, green valley and red sequence (the three populations) we can apply some constraints to these theories.

We have been motivated by a recent result suggesting two contrasting evolutionary pathways through the green valley by different morphological types (Schawinski et al. 2014), specifically that late-type galaxies quench very slowly and form a nearly static disc population in the green valley, whereas early-type galaxies quench very rapidly, transitioning through the green valley and onto the red sequence in ~ 1 Gyr. That study used a toy model to examine quenching across the green valley; here we implement a novel method utilising Bayesian statistics (for a comprehensive overview of Bayesian statistics see either MacKay 2003 or Sivia 1996) in order to find the most likely model description of the star formation histories of galaxies in the three populations. It also provides a direct comparison with our current understanding of galaxy evolution from stellar population synthesis (SPS, see section 3) models.

Through this approach, we aim to determine the following:

(i) What previous star formation history (SFH) causes a galaxy to reside in the green valley at the current epoch?
(ii) Is the green valley a transitional or static population?
(iii) If the green valley is a transitional population then how many routes through it are there?
(iv) Are there morphological dependant differences between these routes through the green valley?

This paper proceeds as follows. Section 2 contains a description of the sample data, which is used in the Bayesian analysis of an exponentially declining star formation history model, all described in Section 3. Section 4 contains the results produced by this analysis, with Section 5 providing a detailed discussion of the results obtained. We also conclude our findings in Section 6. The zero points of all ugriz magnitudes are in the AB system and where necessary we adopt the WMAP Seven-Year Cosmological parameters (Jarosik et al. 2011) with $(\Omega_m, \Omega_\lambda, h) = (0.26, 0.73, 0.71)$.

2 DATA

2.1 Multi-wavelength data

The galaxy sample is compiled from publicly available optical data from the Sloan Digitial Sky Survey (SDSS; York et al. 2000) Data Release 8 (Aihara et al. 2011). Near-ultraviolet (NUV) photometry was obtained from the Galaxy Evolution Explorer (GALEX; Martin et al. 2005) and was matched with a search radius of $1''$ in right ascension and declination.

Observed optical and ultraviolet fluxes are corrected for dust reddening using estimates of internal extinction (Oh et al. 2011) by applying the Cardelli et al. (1989) law. We also adopt k-corrections to $z = 0.0$ from the NYU-VAGC (Blanton et al. 2005; Padmanabhan et al. 2008; Blanton & Roweis 2007) with a typical $u-r$ correction of ~ 0.05 mag. Omitting these corrections does not change the results significantly.

We obtained star formation rates and stellar masses from the MPA-JHU catalog (Kauffmann et al. 2003; Brinchmann et al. 2004; corrected for aperture and extinction), which are in turn calculated from the SDSS spectra and photometry.

We further select a sub-sample with detailed morphological classifications, as described below.

2.2 Galaxy Zoo 2 Morphological classifications

In this investigation we utilise visual classifications of galaxy morphologies from the Galaxy Zoo 2[1] citizen science project (Willett et al. 2013), which obtains multiple independent

[1] `http://zoo2.galaxyzoo.org/`

	All	Red Sequence	Green Valley	Blue Cloud
Smooth-like ($p_s > 0.5$)	42453 (33.6%)	17424 (13.8%)	10687 (8.4%)	14342 (11.3%)
Disc-like ($p_d > 0.5$)	83863 (66.4%)	10722 (8.4%)	13257 (10.5%)	59884 (47.4%)
Early-type ($p_s \geqslant 0.8$)	10517 (8.3%)	5337 (4.2%)	2496 (2.0%)	2684 (2.1%)
Late-type ($p_s \geqslant 0.8$)	51470 (40.9%)	4493 (3.6%)	6817 (5.4%)	40430 (32.0%)
Total	**126316** (100.0%)	28146 (22.3%)	23944 (18.9%)	74226 (58.7%)

Table 1. Table showing the decomposition of the GZ2 sample by galaxy type into the subsets of the colour-magnitude diagram.

classifications for each galaxy image; for which the full question tree for each image is shown in Figure 1 of Willett et al. 2013.

Specifically, the Galaxy Zoo 2 (GZ2) project consists of 304, 022 images from the SDSS DR8 (a subset of those classified in Galaxy Zoo 1; GZ1) all classified by *at least* 17 independent users, with the mean number of classifications standing at ~ 42.The GZ2 sample is more robust than the GZ1 sample and provides more detailed morphological classifications, including features such as bars, the number of spiral arms and the ellipticity of smooth galaxies. It is for these reasons we use the GZ2 sample, as opposed to the GZ1, allowing for further investigation of specific galaxy classes in the future (see Section 5.4). The only selection that was made to the sample was for the removal of objects considered to be stars or artefacts by the users (i.e. with $p_{star/artefact} \geqslant 0.8$). Further to this, we required NUV photometry from the GALEX survey, within which $\sim 42\%$ of the GZ2 sample were observed, giving a total sample size of 126, 316 galaxies.

The first task asks users to chose whether a galaxy is mostly smooth, is featured or is a star/artefact. Unlike other tasks further down in the decision tree, every user who classifies a galaxy image will complete this task (others, such as whether the galaxy has a bar, is dependent on a user having first classified it as a featured galaxy), therefore we have very statistically robust classifications at this level.

The classifications from users produces a vote fraction for each galaxy (the debiased fractions calculated by Willett et al. (2013) were used in this investigation); for example if 80 of 100 people thought a galaxy was disc shaped, whereas 20 out of 100 people thought the same galaxy was smooth in shape (i.e. elliptical), that galaxy would have vote fractions $p_s = 0.2$ and $p_d = 0.8$. In this example this galaxy would be included in the *'clean'* disc sample ($p_d \geqslant 0.8$) according to Willett et al. (2013) and would be considered a late-type galaxy. All previous Galaxy Zoo projects have incorporated extensive analysis of volunteer classifications to measure classification accuracy and biased compute user weightings (for a detailed description of debasing and user-consistency weighting, see Section 3 of Willett et al. 2013).

The classifications are highly accurate and provide a continuous scale of morphological features, as shown in Figure 1, rather than a simple binary classification separating elliptical and disc galaxies. These classifications allow each galaxy to be considered as a probabilistic object with both bulge and disc components. We incorporate this advantage of the GZ classifications into a large statistical analysis of how elliptical and disc galaxies differ in their SFHs; the like of which has not been completed prior to this investigation.

2.3 Defining the Green Valley

To define which of the sample of 126, 316 galaxies were in the green valley, we looked to previous definitions in the literature defining the separation between the red sequence and blue cloud to ensure comparisons can be made with other works. Baldry et al. (2004) used local galaxies from the SDSS to trace this bimodality by fitting double Gaussians to the colour magnitude diagram without cuts in morphology. Their relation is definite in their equation 11 as:

$$C'_{ur}(M_r) = 2.06 - 0.244 \tanh\left(\frac{M_r + 20.07}{1.09}\right) \quad (1)$$

and is shown in Figure 2 by the dashed line. Any galaxy within $\pm 1\sigma$ of this line, shown by the solid lines in Figure 2, is therefore considered a green valley galaxy. The decomposition of the sample into red sequence, green valley and blue cloud galaxies is shown in Table 1 along with further subsections by galaxy type. This table also defines the definitions I adopt henceforth for early-type ($p_s \geqslant 0.8$), late-type ($p_d \geqslant 0.8$), smooth-like ($p_s > 0.5$) and disc-like ($p_d > 0.5$) galaxies.

3 MODELS

3.1 Quenching Models

The quenched star formation history (SFH) of a galaxy can be simply modelled as an exponentially declining star formation rate (SFR) across cosmic time ($0 \leqslant t$ [Gyr] $\leqslant 13.8$) as:

$$SFR = \begin{cases} i_{sfr}(t_q) & \text{if } t < t_q \\ i_{sfr}(t_q) \times exp\left(\frac{-(t-t_q)}{\tau}\right) & \text{if } t > t_q \end{cases} \quad (2)$$

where t_q is the onset time of quenching, τ is the timescale over which the quenching occurs and i_{sfr} is an initial constant star formation rate dependent on t_q. A smaller τ value corresponds to a rapid quench, whereas a larger τ value corresponds to a slower quench.

We assume that all galaxies formed at a time $t = 0$ Gyr with an initial burst of star formation. The mass of this initial burst is controlled by the value of the i_{sfr} which is set

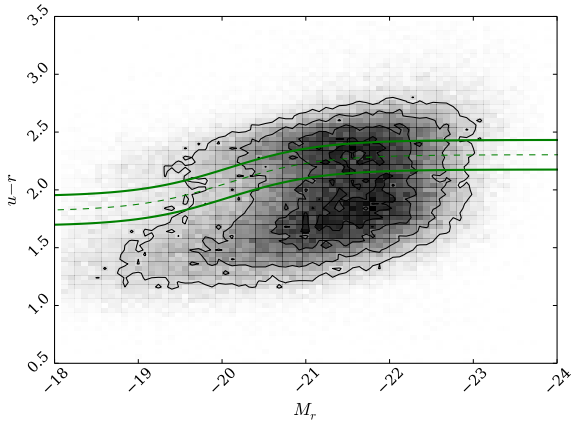

Figure 2. Colour-magnitude diagram for the Galaxy Zoo 2 population showing the definition between the blue cloud and the red sequence from Baldry et al. (2004) with the dashed line. The solid lines show $\pm 1\sigma$ either side of this definition; any galaxy within the boundary of these two solid lines is considered a green valley galaxy.

as the average sSFR at the time of quenching t_q. Peng et al. (2010) defined a relation (their equation 1) by empirically fitting to SDSS data for the average sSFR and redshift (cosmic time, t) as:

$$sSFR(m,t) = 2.5\left(\frac{m}{10^{10}M_{\odot}}\right)^{-0.1}\left(\frac{t}{3.5}\right)^{-2.2}\mathrm{Gyr}^{-1}. \quad (3)$$

Beyond $z \sim 2$ the characteristic SFR flattens and is roughly constant back to $z \sim 6$. The cause for this change is not well understood but can be seen across similar observational data (Peng et al. 2010; González et al. 2010; Béthermin et al. 2012). Motivated by these observations, the relation defined in Peng et al. (2010) is taken up to a cosmic time of $t = 3$ Gyr(z ~ 2.3) and prior to this a constant average SFR is assumed (see Figure 6). At the point of quenching, t_q, the models are defined to have a SFR which lies on this relationship for the sSFR, for a galaxy with mass, $m = 10^{10.27}M_{\odot}$ (the mean mass of the GZ2 sample; see Figure 6.

Under these assumptions the average SFR of our models will result in a lower value than the relation defined in Peng et al. (2010) at all cosmic times with this treatment; each galaxy only resides on the 'main sequence' at the point of quenching. However galaxies cannot remain on the 'main sequence' from early to late times throughout their entire lifetimes given the unphysical stellar masses and SFRs this would result in at the current epoch in the local Universe (Béthermin et al. 2012; Heinis et al. 2014). If we were to include prescriptions for no quenching, starbursts, mergers, AGN etc. into our models we would improve on our reproduction of the average SFR across cosmic time; however we chose to initially focus on the most simple model possible.

Once this evolutionary SFR is obtained, it is convolved with the Bruzual & Charlot (2003) population synthesis models to generate a model SED at each time step. The observed features of galaxy spectra can be modelled using simple stellar population techniques which sum the contributions of individual, coeval, equal-metallicity stars. The accuracy of these predictions depends on the completeness of the input stellar physics. Comprehensive knowledge is therefore

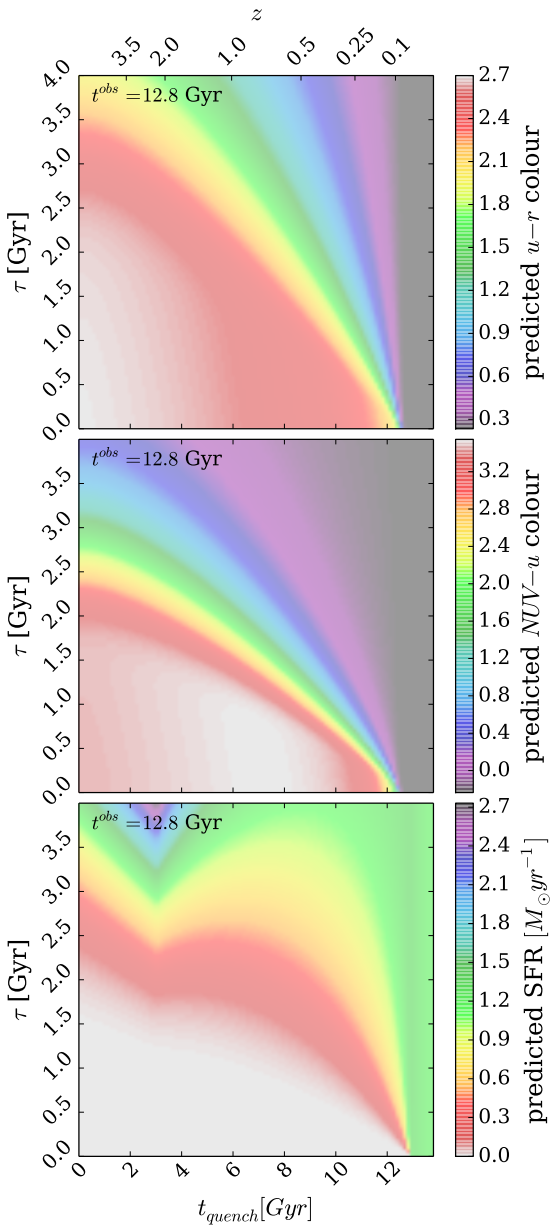

Figure 3. Quenching timescale τ versus quenching onset time t in all three panels. Colour shadings show model predictions of the $u-r$ optical colour (top panel), $NUV-u$ colour (middle panel), and star formation rate in $M_{\odot}$ yr^{-1} (lower panel), at $t^{obs} = 12.8$ Gyr, the mean 'observed' time of the GZ2 sample. The combination of optical and NUV colours is a sensitive measure of the $\theta = [t_q, \tau]$ parameter space. Note that all models with $t > 12.8$ Gyr are effectively un-quenched. The 'kink' in the bottom panel is due to the assumption that the sSFR is constant prior to $t \sim 3$ Gyr ($z \sim 2.2$).

required of (i) stellar evolutionary tracks and (ii) the initial mass function (IMF) to synthesise a stellar population accurately. These stellar population synthesis (SPS) models are an extremely well explored (and often debated) area of astrophysics (Maraston 2005; Eminian et al. 2008; Conroy, Gunn & White 2009; Falkenberg et al. 2009; Chen et al. 2010; Kriek et al. 2010; Miller, Rose & Cecil 2011; Mel-

bourne et al. 2012). In this investigation we chose to utilise the Bruzual & Charlot (2003) *GALEXEV* SPS models along with a Chabrier (Chabrier et al. 2003) IMF, across a large wavelength range ($0.0091 < \lambda\,[\mu\mathrm{m}] < 160$), at solar metallically (m62 in the Bruzual & Charlot (2003) models), across cosmic time.

We choose the Bruzual & Charlot (2003) stellar population synthesis models over the Maraston (2005) models due to their proven reliability in reproducing colours of 'typical' galaxies. Maraston (2005) focus on improving the implementation of TP-AGB stars in these models, which are known to severely redden post-starburst populations (Marigo & Girardi 2007; Kriek et al. 2010). Given that we are investigating a quenching star formation history model, rather than a starburst, we feel that the Bruzual & Charlot (2003) models are more appropriate for this investigation.

Fluxes from stars younger than 3 Myr in the SPS model are suppressed to mimic the large optical depth of protostars embedded in dusty formation cloud (as in S14), then filter transmission curves are applied to the fluxes to obtain AB magnitudes and therefore colours. The right panel of Figure 6 shows the evolution of these colours from the point of quenching onwards in the optical-NUV colour space. Given that information about these modelled populations is available across all cosmic time, they can be 'observed' at a given time in their history t^{obs}; this correlates with the observed redshift of the GZ2 sample given the modelling assumptions. Therefore, for the GZ2 sample, the observed redshift was used to calculate the assumed age of each galaxy, in order to compare the observed colours to the predicted models colours directly.

Figure 3 shows these predicted optical and NUV colours at a time of $t^{obs} = 12.8$ Gyr (the average observed time of the Galaxy Zoo 2 sample, $z \sim 0.076$) provided by the exponential SFH model. These predicted colours will be referred to as $d_{c,p}(t_q, \tau, t^{obs})$, where c={opt,NUV} and p = predicted. The SFR at a time of $t^{obs} = 12.8$ Gyr is also shown in Figure 3 to compare how this correlates with the predicted colours. The $u-r$ predicted colour shows an immediate correlation with the SFR, however the $NUV-u$ colour is more sensitive to the value of τ and so is ideal for tracing any recent star formation in a population . At small τ (rapid quenching timescales) the $NUV-u$ colour is insensitive to t_q, whereas at large τ (slow quenching timescales) the colour is very sensitive to t_q. Together the two colours are ideal for tracing the effects of t_q and τ in a population.

3.2 Bayesian Techniques

In order to achieve robust conclusions we conduct a a fully Bayesian analysis (Sivia 1996; MacKay 2003) of our SFH models in comparison to the observed GZ2 sample data. This approach requires consideration of all possible combinations of $\theta \equiv (t_q, \tau)$. Assuming that all galaxies formed at $t = 0$ Gyr with an initial burst of star formation, we can assume that the 'age' of each galaxy in the GZ2 sample is equivalent to an observed time, t_k^{obs} (see Section 2.2). We then use this 'age' to calculate the predicted model colours at this cosmic time for a given combination of θ: $d_{c,p}(\theta, t_k^{obs})$ for both optical and NUV ($c = opt, NUV$) colours. We can now directly compare our model colours with the observed GZ2 galaxy colours, so that for a single galaxy k with optical

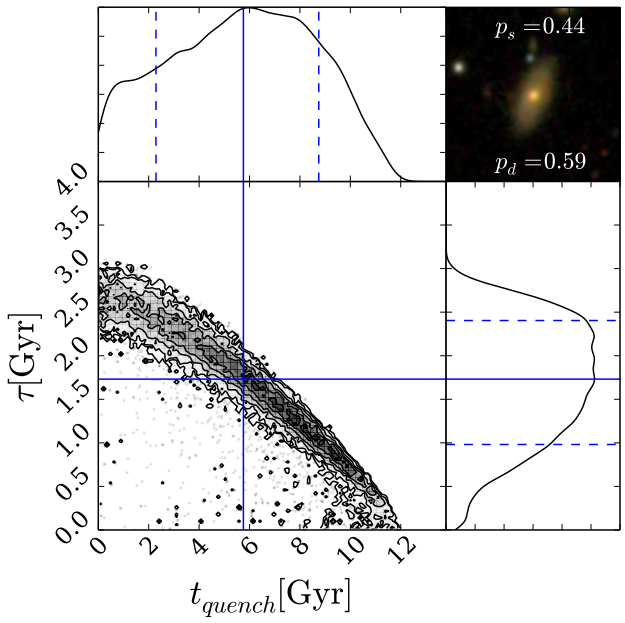

Figure 4. Example output from *StarfPy* for a galaxy within the red sequence. The contours show the positions of the 'walkers' in the Markov Chain (which are analogous to the areas of high probability) for the quenching models described by $\theta = [t_q, \tau]$ and the histograms show the 1D projection along each axis. Solid (dashed) blue lines show the best fit model (with $\pm 1\sigma$) to the galaxy data. The postage stamp image from SDSS is shown in the top right along with the vote fractions for smooth (p_s) and disc (p_d) from Galaxy Zoo 2.

$(u-r)$ colour, $d_{opt,k}$ and NUV $(NUV-u)$ colour, $d_{NUV,k}$, the likelihood $P(d_k|\theta, t_k^{obs})$ is:

$$P(d_k|\theta, t_k^{obs}) = \frac{1}{\sqrt{2\pi\sigma_{opt,k}^2}} \frac{1}{\sqrt{2\pi\sigma_{NUV,k}^2}} \exp\left[-\frac{(d_{opt,k} - d_{opt,p}(\theta, t_k^{obs}))^2}{\sigma_{opt,k}^2}\right] \exp\left[-\frac{(d_{NUV,k} - d_{NUV,p}(\theta, t_k^{obs}))^2}{\sigma_{NUV,k}^2}\right], \quad (4)$$

We have assumed that $P(d_{opt}|\theta, t_k^{obs})$ and $P(d_{NUV}|\theta, t_k^{obs})$ are independent of each other and that the errors on the observed colours are also independent. To obtain the probability of each combination of θ values given the GZ2 data: $P(\theta|\underline{d}, t^{obs})$, i.e. how likely is a single SFH model given the observed colours of a single GZ2 galaxy, we utilise Bayes' theorem:

$$P(\theta|d_k) = \frac{P(d_k|\theta, t^{obs})P(\theta)}{\int P(d_k|\theta, t^{obs})P(\theta)d\theta}. \quad (5)$$

We assume a flat prior on the model parameters so that:

$$P(\theta) = \begin{cases} 1 & \text{if } 0 \leqslant t_q \leqslant 13.8 \text{ and } 0 \leqslant \tau \leqslant 4 \\ 0 & \text{otherwise} \end{cases} \quad (6)$$

As the denominator of Equation 5 is a normalisation

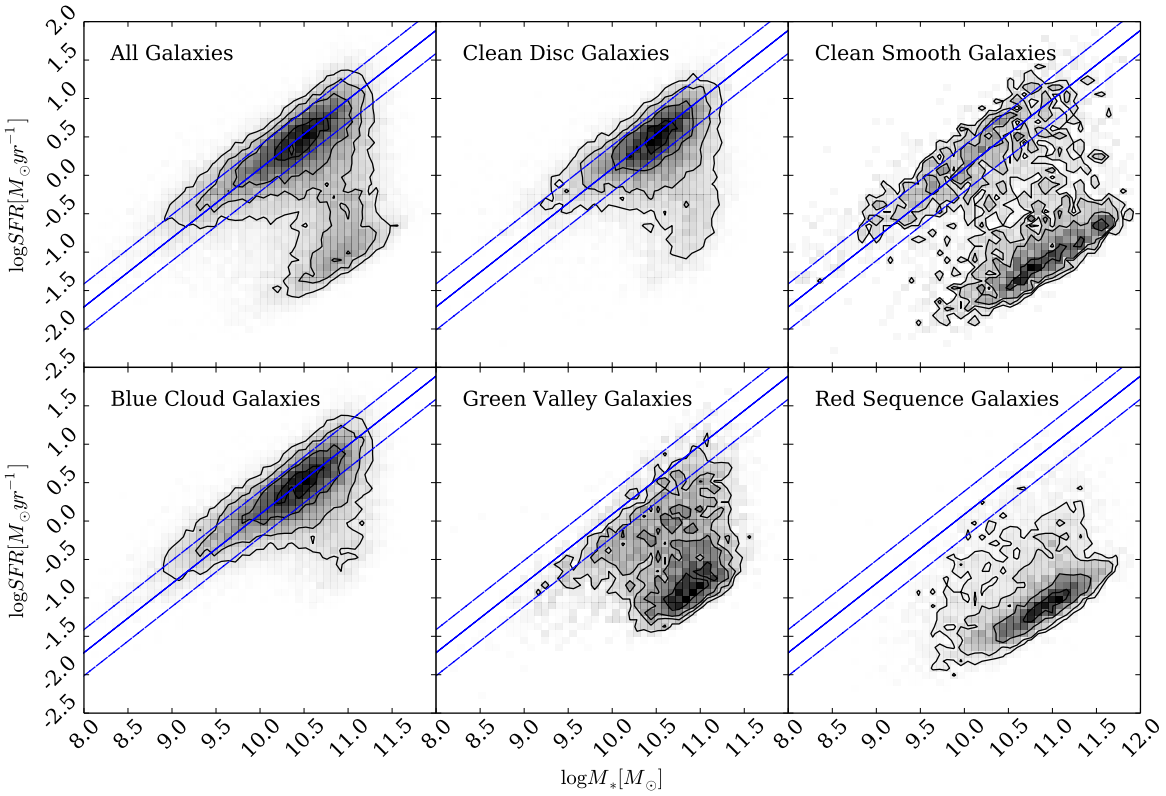

Figure 5. Star formation rate versus stellar mass diagrams show how the different populations of galaxies (top row, left to right: all galaxies, GZ2 'clean' disc and smooth galaxies; bottom row, left to right: blue cloud, green valley and red sequence galaxies) contribute to the star forming sequence (from Peng et al. (2010), shown by the solid blue line with 0.3 dex scatter by the dashed lines) of star formation. Based on positions in these diagrams, the green valley does appear to be a transitional population between the blue cloud and the red sequence. Detailed analysis of star formation histories can elucidate the nature of the different populations' pathways through the green valley. The clean smooth and disc samples are described in 2.2.

factor, comparison between likelihoods for two different SFH models (i.e., two different combinations of $\theta = (t_q, \tau)$) is equivalent to a comparison of the numerators. Calculation of $P(\theta|\underline{d}, \underline{t}, ^{obs} w)$ for any θ is possible given data for the GZ2 sample (or a sub-sample thereof). Markov Chain Monte Carlo (MCMC; MacKay 2003; Foreman-Mackey et al. 2013; Goodman & Weare 2010) provides a robust comparison of the likelihoods between θ values; here we choose a Python implementation of an affine invariant ensemble sampler by Foreman-Mackey et al. (2013); *emcee*.

This method allows for a more efficient exploration of the parameter space by avoiding those areas with low likelihood. A large number of 'walkers' are started at an initial position where the likelihood is calculated; from there they individually 'jump' to a new area of parameter space. If the likelihood in this new area is greater (less) than the original position then the 'walkers' accept (reject) this change in position. Any new position then influences the direction of the 'jumps' of other walkers. This is repeated for the defined number of steps after an initial 'burn-in' phase. *emcee* returns the positions of these 'walkers', which are analogous to the regions of high probability in the model parameter space. The model outlined above has been coded using the *Python* programming language into a package named: *StarfPy* which has been made freely available to download[2]. An example output from this Python package for a single galaxy from the GZ2 sample in the red sequence is shown in Figure 4. The contours show the positions of the 'walkers' in the Markov Chain which are analogous to the areas of high probability.

We wish to consider the model parameters for the populations of galaxies across the colour magnitude diagram for both smooth and disc galaxies, therefore we run the *StarfPy* package on each galaxy in the GZ2 sample. This was extremely time consuming; for each combination of θ values which *emcee* proposes, a new SFH must be built prior to convolving it with the BC03 SPS models at the observed age and then predicted colours calculated from the resultant SED. For a single galaxy this could take up to 2 hours on a typical desktop machine for long Markov Chains. A look-up table was therefore generated at 50 t^{obs} for 100 t_{quench} and 100 τ values; this was then interpolated over for a given observed galaxy's age and proposed θ values at each step in the Markov Chain. This ensured that a single galaxy took 2 minutes to run on a typical desktop machine. This interpolation was found to incorporate an error of ± 0.1 into the quoted best fit θ values (see Appendix section **??** for further information).

[2] github.com/rjsmethurst/starfpy

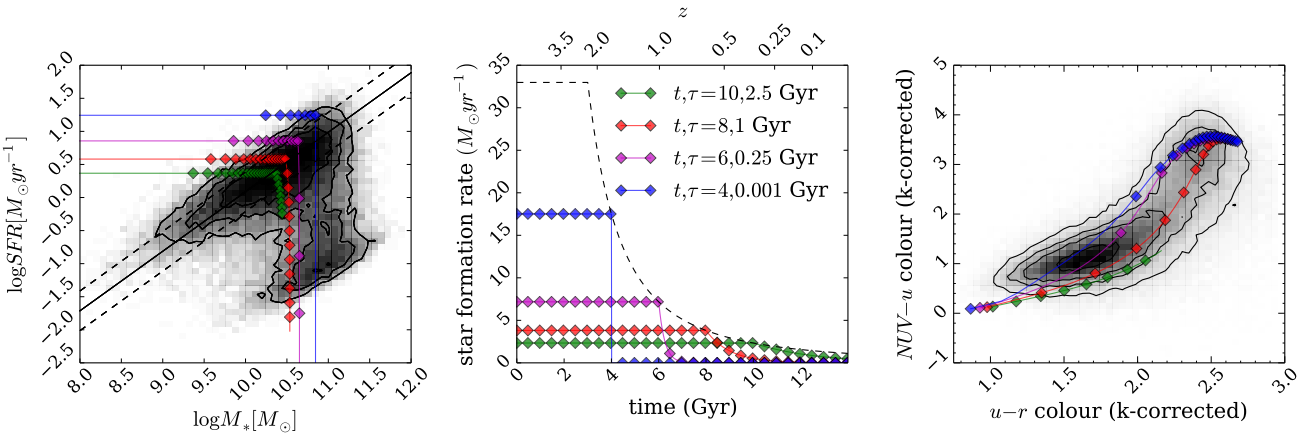

Figure 6. Left panel: SFR vs. $M_*$for all 126,316 galaxies in our full sample (shaded contours), with model galaxy trajectories shown as coloured points/lines. The SFHs of the models are shown in the middle panel, where the SFR is initially constant before quenching at time t and thereafter exponentially declining with a characteristic timescale τ. We set the SFR at the point of quenching to be consistent with the typical SFR of a star-forming galaxy at the quenching time, t (dashed line; Peng et al. 2010). The full range of models reproduces the observed colour-colour properties of the sample (right panel); for clarity the figures show only 4 of the possible models explored in this study.

Using this lookup table, each of the 126, 316 total galaxies in the GZ2 sample was run through *StarfPy* on multiple cores of a computer cluster to obtain the Markov Chain positions (analogous to $P(\theta|d_k)$) for each galaxy, k (see Figure 4). In each case the Markov Chain consisted of 100 'walkers' which took 400 steps in the 'burn-in' phase and 400 steps thereafter at which point the acceptance fraction was checked to be within the range $0.25 < f_{acc} < 0.5$ (which was true in all cases). These individual galaxy positions are then combined to give the areas of high probability in the model parameter space across a given population (e.g. the green valley). We compute this by first discarding positions with a corresponding probability of $P(\theta|d_k) < 0.2$ in order to exclude galaxies which are not well fit by the quenching model; for example blue cloud galaxies which are still star forming will be poorly fit by a quenching model. The positions are then binned and weighted by their corresponding probability $P(\theta|d_k)$. The GZ2 data also provides uniquely powerful continuous measurements of a galaxy's morphology, therefore we utilise the user vote fractions to obtain separate model parameters for both smooth and disc galaxies. This is obtained by also weighting by the morphology vote fraction when the binned positions are summated, as follows:

$$P(\theta_{disc}|\underline{d}) = \frac{1}{Z}\sum_k p_{disc,k} P(\theta|d_k), \quad (7)$$

and

$$P(\theta_{smooth}|\underline{d}) = \frac{1}{Z}\sum_k p_{smooth,k} P(\theta|d_k), \quad (8)$$

where Z is a normalisation constant. For example, the galaxy shown in Figure 4 would contribute almost evenly to both the smooth and disc parameters by the vote fractions. Since galaxies with similar vote fractions contain both a bulge and disc component, this method is effective in incorporating intermediate galaxies which are thought to be crucial to the morphological changes between early- and late-type galaxies. It was the consideration of these intermediate galaxies which was excluded from the investigation by S14.

4 RESULTS

Figure 5 shows the SFR versus the stellar mass for the observed GZ2 sample which has been split into blue cloud, green valley and red sequence populations as well as into the 'clean' disc and smooth galaxy samples (with GZ2 vote fractions of $p_d \geqslant 0.8$ and $p_s \geqslant 0.8$ respectively). The green valley galaxies are indeed a population which have either left, or begun to leave, the SFR-mass relation or have some residual star formation still occurring. Interestingly, when we compare those galaxies which reside on the star forming sequence we find that the tail ends of this population (the low and high mass galaxies) are primarily made up of smooth galaxies as opposed to disc galaxies.

The left panel in Figure 6 shows how well the quenching models reproduce the observed relationship between the SFR and the mass of a galaxy, including how at the time of quenching they reside on the star forming sequence shown by the solid black line for a galaxy of mass, $M = 10^{10.27} M_\odot$.

These models were implemented in the *StarfPy* package to produce Figures 7, 8 & 9 for the red sequence, green valley and blue cloud populations of smooth and disc galaxies respectively. In this Section we refer to rapid, intermediate and slow quenching timescales which correspond to ranges of τ [Gyr] < 1.0, $1.0 < \tau$ [Gyr] < 2.0 and τ [Gyr] > 2.0 respectively.

4.1 Red Sequence Galaxies

The left hand panel of Figure 7 reveals that smooth galaxies found in the optical red sequence show a preference (51.1%) for rapid quenching timescales across all cosmic time. Figure 7 shows us that the typical smooth, red sequence galaxy has undergone a SFH with a rapid to intermediate quench at

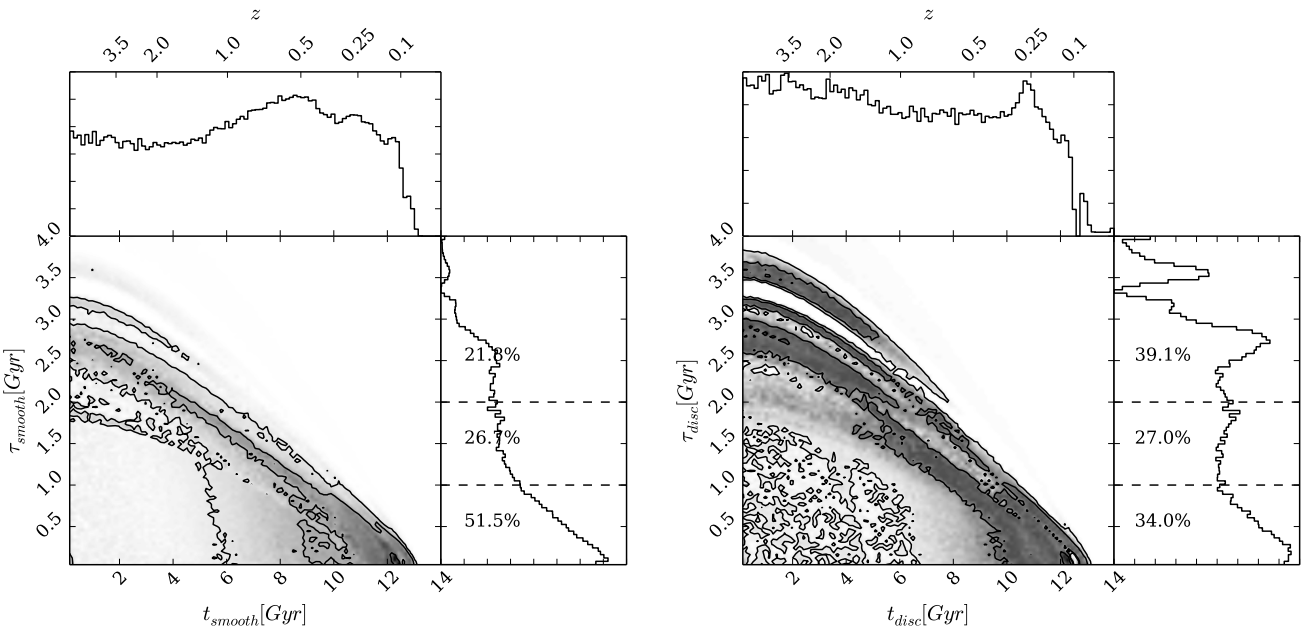

Figure 7. Contor plots showing the cumulative positions in the Markov Chain for galaxies in the red sequence, weighted by the morphological vote fractious from GZ2 to give the areas of high probability in the model parameter space for both bulge (left) and disc (right) dominated systems. The histograms show the projections into one dimension for each parameter. The dashed lines show the separation between rapid (τ [Gyr] < 1.0), intermediate ($1.0 < \tau$ [Gyr] < 2.0) and slow (τ [Gyr] > 2.0) quenching timescales with the percentage probability in each section.

various times, resulting in a very low current SFR. These are therefore the typical *'red and dead'* galaxies expected to be found in the red sequence.

For the smooth parameters in the left panel of Figure 7 we also have preference for slow and intermediate quenching timescales but only at early times. Perhaps this is the influence of intermediate galaxies (with $p_s \sim p_d \sim 0.5$), hence why similar high likelihood areas exist for both the smooth-like and disc-like galaxies and considering there are far more of these intermediate galaxies than those that are definitively early- or late-types (see Table 1). These galaxies are those whose morphology cannot easily be distinguished or deliberated either because it is at a large distance or because it is an S0 galaxy whose morphology can be deliberated by different users in different ways. Willett et al. (2013) find that the S0 galaxies expertly classified by Nair & Abraham (2010) are more commonly classified as ellipticals by GZ2 users have a significant tail to high disc vote fractions, giving a possible explanation as to the origin of this low level area of probability.

The rapid quenching timescales are dominant especially in smooth galaxies back to $z \sim 1$ prior to which intermediate and slower quenching timescales are the preferred mode. If we take into account the observed peak of average star formation rate in the Universe, which has been found to occur at $z \sim 2$ (Hopkins 2004) we can assume that when more SF is occurring, quenching is a more difficult task. We can see that after $z \sim 2$ the preference for quenching begins to rise (top histogram in the left hand panel of Figure 7), coinciding with the decline in the average star formation.

The right hand panel of Figure 7 reveals that disc galaxies show almost equal preference for rapid (34.0%) and slow (39.1%) quenching timescales. This preference for very slow quenching timescales (the like of which are not seen in either the green valley or blue cloud, see Figures 8 and 9) suggests that these galaxies have only just reached the red sequence after a very slow evolution across the colour-magnitude diagram. Considering their limited number it is likely that these galaxies are currently on the edge of the red sequence having recently (and finally) moved out of the green valley. Table 1 shows that 3.9% of our sample are red sequence clean disc galaxies, i.e. red late-type spirals, this is, within error, in agreement with the findings of Masters et al. (2010a) who find $\sim$ 6% of late-type spirals are red when defined by a cut in the $g - r$ optical colour at the 'blue end of the red sequence' (rather than with $u - r$ as implemented in this investigation).

The disc galaxies also show equal preference for rapid as for slow quenching timescales, however only at recent times, which is contradictory to the findings of S14. This could again be due to the intermediate galaxies, however since the percentages in Figure 7 are similar for rapid and slow quenching timescales, unlike in the smooth galaxies, this suggests some other underlying mechanism that affects these disc galaxies. Perhaps these rapid quenching timescales can also be attributed to a morphological change, suggesting that the quenching has occurred more rapidly than the morphological change to a bulge dominated system in these disc galaxies.

The top histogram in the right hand panel shows us that the the quenching is distributed evenly over cosmic time. Downsizing has only ever been observed in elliptical galaxies (*Thomas et al?? - needs a reference*) therefore this constant

quenching confirms the assumption that whatever is driving the evolution of discs is constant over cosmic time.

We also compare the resultant SFRs for both the smooth- and disc-like galaxies in Figure 7 by noticing where the areas of high probability lie with respect to the bottom panel of Figure **??** which shows the predicted SFR at an observation time of $t \sim 12.8$ Gyr (the average observed time of the GZ2 population) across the parameter space. We can see that those red sequence disc galaxies with a preference for slow quenching still have some residual star formation occurring, SFR$\sim 0.105 M_{\odot} yr^{-1}$, whereas the smooth galaxies with a preference for rapid quenching have a resultant SFR$\sim 0.0075 M_{\odot} yr^{-1}$. This is approximately 14 times less than the residual SFR still occurring in the red sequence disc galaxies. Within error, this is in agreement with the findings of Tojeiro et al. (2013) who, by using the Versatile Spectral Analyses spectral fitting code, found that red late-type spirals show 17 times more recent star formation than red elliptical galaxies.

These results for red sequence galaxies have many implications for green valley galaxies, as all of these systems must have passed through this region on their way to the red sequence. Therefore if the green valley is a transitional population we expect to see a similar distribution of likelihoods for the green valley disc-like and smooth-like galaxies but perhaps at later quenching times, pre-empting what will become the red sequence over time.

4.2 Green Valley Galaxies

In Figures 8 and **??** we can make similar comparisons for the green valley galaxies to those discussed previously for the red sequence. In Figure 8 we still see the correlation between the two parameters as seen in Figure **??** but the areas of high likelihood for the parameters have changed. We no longer have a trimodal or bimodal likelihood in the parameter space for smooth or disc galaxies respectively.

Among green valley galaxies there is little to no likelihood for rapid quenching timescales regardless of morphology. Quenching in the green valley also occurs on similar timescales, τ to that of the red sequence, but at more recent times t; hence they have some higher recent star formation than the other galaxies in the blue cloud. There is a very little likelihood however, for rapid quenching of the smooth-like galaxies. This may be counter intuitive at first, as one of the main arguments for the lack of galaxies in the green valley is due to the hypothesised rapid movement across it; however the proportion of present day green valley galaxies with this history will therefore be lower. Especially considering the number of intermediate galaxies which are present in the green valley compared to those that are in the clean samples. These galaxies will be overwhelming the 'walker' positions in the algorithm.

Therefore if we remove the influence of such galaxies as in Figure **??**, which shows the regions of high likelihood for the model parameters for only the 'clean' green valley galaxies, we can see that we do indeed detect some very rapid quenching at very recent times. However we only find this for smooth galaxies, just as in Figure **??** suggesting again that it is only early-type galaxies which can progress through the green valley and into the red sequence in such a way.

For the clean disc galaxies, whose parameters were also overwhelmed by the sheer number of intermediate galaxies in the green valley, we can see a large shift in likelihood in the right panel of Figure **??** from those in Figure 8. Upon removal of the intermediate galaxies the regions of high likelihood now reside at much longer quenching timescales, as expected for a late-type galaxy. We still have some likelihood for galaxies with higher SFR than the other galaxies, suggesting there are also some late-type galaxies that have just progressed from the blue cloud into the green valley.

Given enough time ($t \sim 4 - 5$Gyr), these clean disc galaxies will eventually fully pass through the green valley and make it out to the red sequence (the right panel of Figure 6 shows galaxies with $\tau > 1.0$ Gyr do not approach the red sequence within 3 Gyr post quench). This is most likely the origin of the 'red spirals'. We therefore theorise that with enough cosmic time, eventually disc-like galaxies will come to populate the red sequence at comparable fractions to smooth-like galaxies. At our current epoch and at the timescales at which disc-like galaxies have a high likelihood we would not expect to see a large number of red disc-like galaxies.

By comparing Figure **??** with Figure **??**, we can see that the parameters occupy similar regions of space in the τ parameter but have gained a shift to later times in the t parameter, for both types of morphology. This means that both populations are tracing the evolution of the red sequence, confirming that green valley is indeed a transitional population between blue cloud and red sequence regardless of morphology. Currently as we observe the green valley, its main constituent, are very slowly evolving disc-like galaxies along with intermediate- and some smooth-like galaxies which manage to pass across it within $\sim 1.0 - 1.5$ Gyr.

All of this evidence suggests that there are not just two routes for galaxies through the green valley but *three*: with the smooth- ($1.0 < \tau < 1.5$ Gyr), intermediate- ($1.5 < \tau < 2.0$ Gyr) and disc-like ($\tau > 2.0$ Gyr) galaxies each having different SFHs which lead them across the green valley, given enough cosmic time. Since S14 did not consider intermediate galaxies, their conclusions that there are 2 routes through the green valley for galaxies contradicts with our statements that their are three or more routes, dependant on whether a galaxy is early-, intermediate- or late-type.

4.3 Blue Cloud Galaxies

Since the blue cloud is considered to be primarily made of star forming galaxies we expect the model to have some difficulty in determining the most likely quenching model to describe them. In Figure 9 both sets of parameters show high likelihood for slow quenching at late times, with a higher likelihood for the disc-like galaxies. We believe that this is the model picking up on those galaxies which have so far not undergone any quenching, as this is the only way it can account for the observed blue optical and NUV colours of these galaxies (at this point we remind the reader that although a galaxy has undergone quenching, star formation can still be occurring in a galaxy, just at a slower rate than at an earlier time).

However we also see a bimodality in both sets of parameters (see Figure 9), from these recent, slow quenches (i.e. minimal drop in SFR) to intermediate quenching timescales

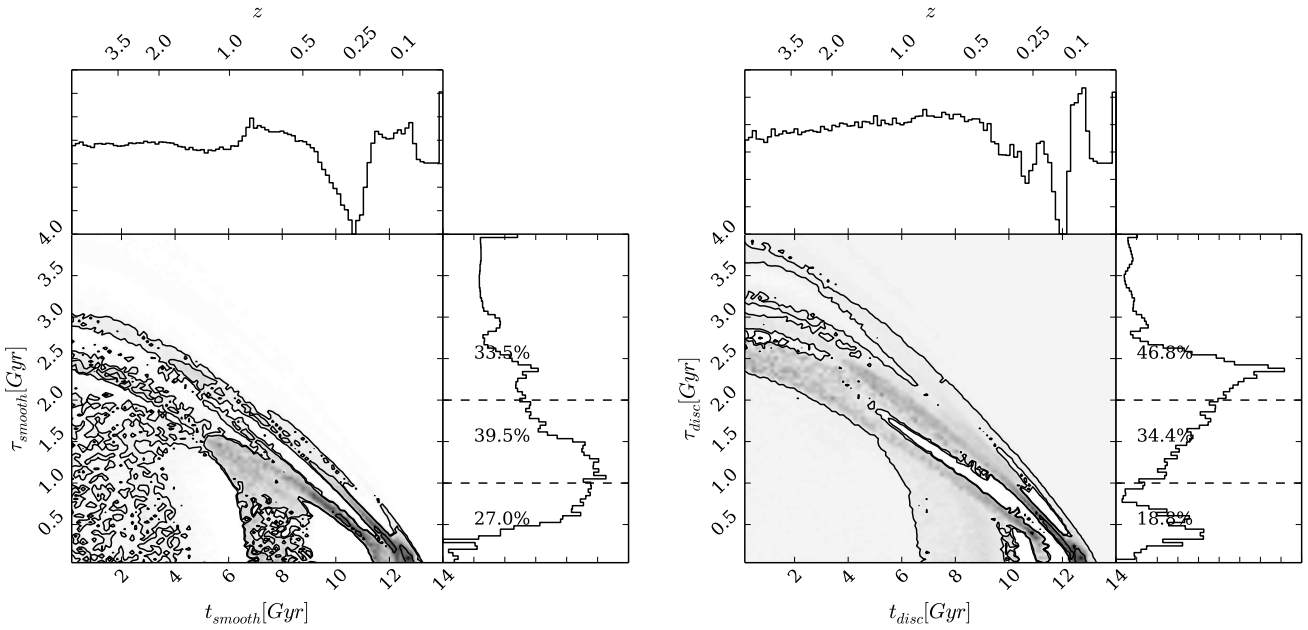

Figure 8. Contor plots showing the cumulative positions in the Markov Chain for galaxies in the green valley, weighted by the morphological vote fractious from GZ2 to give the areas of high probability in the model parameter space for both bulge (left) and disc (right) dominated systems. The histograms show the projections into one dimension for each parameter. The dashed lines show the separation between rapid (τ [Gyr] < 1.0), intermediate ($1.0 < \tau$ [Gyr] < 2.0) and slow (τ [Gyr] > 2.0) quenching timescales with the percentage probability in each section.

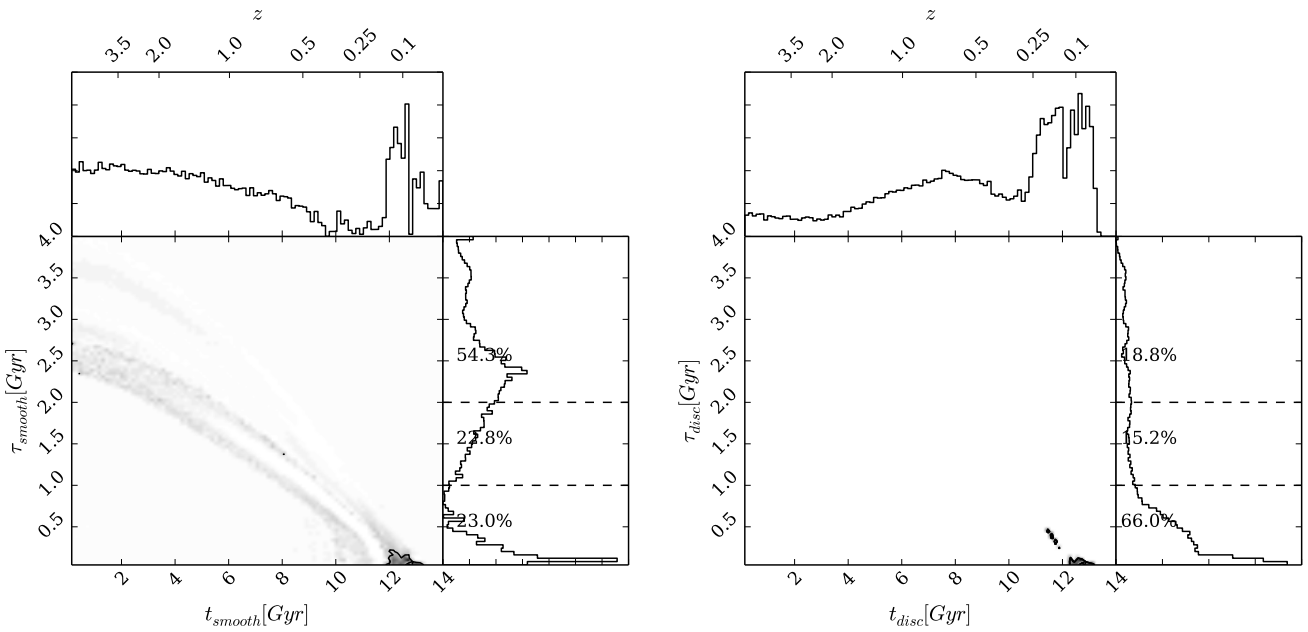

Figure 9. Contor plots showing the cumulative positions in the Markov Chain for galaxies in the blue cloud, weighted by the morphological vote fractious from GZ2 to give the areas of high probability in the model parameter space for both bulge (left) and disc (right) dominated systems. The histograms show the projections into one dimension for each parameter. The dashed lines show the separation between rapid (τ [Gyr] < 1.0), intermediate ($1.0 < \tau$ [Gyr] < 2.0) and slow (τ [Gyr] > 2.0) quenching timescales with the percentage probability in each section. Positions with probabilities less than 0.2 are discarded as poorly fit models, therefore we can conclude unsurprisingly that blue cloud galaxies are not well described by a quenching star formation model.

from $t \sim 9$ Gyr which is more pronounced in the disc-like galaxies. This suggests that there is quenching occurring within the blue cloud (the likelihood for which is higher for the disc galaxies); suggesting that those galaxies which have begun to quench in the blue cloud are already tracing the parameters of the green valley. This confirms once more that the green valley is a transitional population between the blue cloud and red sequence regardless of morphology.

We note that in this case there is no rapid quenching for either population, confirming, as expected, that any galaxy undergoing a rapid quench will very quickly leave the blue cloud.

The SFH parameter space for the smooth-like and disc-like galaxies also appear very similar, suggesting galaxies in the blue cloud are very similar regardless of their morphology. Of all of the regions of the CMD, this is to be expected in the blue cloud since it consists of galaxies that are predominantly still star forming, confirmed by the inability of the model to attribute the extremely blue colours of the majority of these galaxies to slow quenching at recent times (i.e. very little change in the SFR; see Figures 9 and **??**). The way these galaxies must therefore differ, is in the mechanisms and triggers by which they have formed their stars, having no effect on the observed colours, but a discernible effect on their morphologies.

When we compare Figures 9 and **??** which shows the likely model parameters for the all and the 'clean' blue cloud galaxies; the smooth- and disc-like galaxies both have high likelihood for a slow quench model at late times and the clean disc galaxies have a high likelihood for any timescale of quenching at late times. This suggests that most galaxies in the GZ2 sample residing in the blue cloud still have star formation occurring.

When we compare the left and right panels of Figure **??** we still retain some preference for intermediate quenching at recent times for the disc galaxies (which we do not for the smooth parameters), suggesting that the blue cloud is primarily composed of both star forming disc and smooth galaxies and disc galaxies which have been quenched with intermediate timescales slowly moving across the colour-magnitude diagram.

Clean blue cloud smooth galaxies have high likelihoods clustered only at late times with slow quenching timescales where the bluest colours are predicted by the models. This suggests that these galaxies have not undergone any quenching and cannot accurately be described by our quenching model. This therefore leads to theories for blue ellipticals as either merger-driven or gas inflow driven reinvigorated star formation.

5 DISCUSSION

We have implemented a Bayesian statistic analysis of the star formation histories (SFHs) of a large sample of galaxies classified by Galaxy Zoo. We have found differences between the SFHs of smooth- and disc-like galaxies across the colour-magnitude diagram in the red sequence, green valley and blue cloud. In this section we will speculate on what are the possible mechanisms driving this difference?

5.1 Rapid Quenching Mechanisms

There is a lack of likelihood for rapid quenching timescales $\tau < 1.0$ Gyr across all subsets of galaxies. This is most apparent in the disc parameters (the right hand panels of Figures **??** - **??**) where no likelihood below this is detected; except at very recent times for the clean disc blue cloud galaxies. For the smooth galaxies a small amount of likelihood is found for these extremely rapid quenching timescales, suggesting the mechanism which drives this quenching is not only less likely than intermediate quenching, but that it only occurs for smooth-like galaxies (this is in agreement with the findings of S14, however they attribute this rapid quenching as the most common mechanism for smooth galaxies). This suggests that this rapid quenching mechanism causes a change in morphology from a disc- to a smooth-like galaxy as it traverses the colour-magnitude diagram from the blue cloud to the red sequence. It seems plausible therefore, that this rare, rapid quenching mechanism is due to major mergers of equal mass galaxies.

Inspection of the galaxies contributing to this area of likelihood reveals that this does not arise due to currently merging pairs identified by GZ users, but by typical smooth galaxies with red optical and NUV colours that the model attributes to rapid quenching at early times.

One simulation of interest by Springel, Di Matteo & Hernquist (2005) showed that feedback from black hole activity is a necessary component of destructive major mergers to produce such rapid quenching timescales. Powerful quasar outflows remove much of the gas from the inner regions of the galaxy, terminating star formation on extremely short timescales. Bell et al. (2006) using data from the COMBO-17 redshift survey ($0.4 < z < 0.8$)estimate a merger timescale from being classified as a close galaxy pair and recognisably (i.e. morphologically) disturbed as ~ 0.4 Gyr and Springel, Di Matteo & Hernquist (2005) consequently find using hydrodynamical simulations that after ~ 1 Gyr the merger remanent has reddened to $u - r \sim 2.0$. This is in agreement with the predictions of our models which show in Figure 6 that within ~ 1 Gyr (each point represents a time step of 0.5 Gyr) the models with $\tau < 0.4$ Gyr have reached the red sequence with $u - r \gtrsim 2.2$.

We can also compare our predictions for the fractions of clean red sequence galaxies which have undergone such a rapid quenching star formation history, to the predicted merger fraction from observations and simulations. We find that of the galaxies in our sample that are defined as both clean and residing within the red sequence, $\sim 4.2\%$ of them have a preferred likelihood for models with $\tau < 0.4$ Gyr. This is in agreement with the observations by Bell et al. (2006) who showed that $5\% \pm 1\%$ of massive galaxies (with $M_* > 2.5 \times 10^{10} M_\odot$) are in a close galaxy pair and of Bundy et al. (2009) who found that the fraction of systems resulting in a major merger was 4%, and that this fraction did not change significantly with redshift.

Most of this rapid quenching occurs for smooth galaxies in the red sequence (see Figure **??**) and it occurs before a quenching time of $t \sim 6$ Gyr ($z \sim 1$). This is in agreement with Im et al. (2002) who state that if major mergers are responsible for the formation of luminous ellipticals (and S0s) such a process must have occurred predominantly before ($z \sim 1$).

We reiterate that this rapid quenching mechanism is very rare for smooth galaxies and even rarer for discs. Dry major mergers therefore do not fully account for the formation of any galaxy type at any redshift, supporting the observational conclusions made by Bell et al. (2007); Bundy et al. (2007); Kaviraj (2014) and simulations by Genel et al. (2008).

5.2 Intermediate Quenching Mechanisms

Intermediate quenching timescales are found to be the most dominant quenching rough for both smooth and disc galaxies at various different quenching times. This intermediate quenching route must therefore be possible with routes that both preserve and transform morphology. It is this result that is in disagreement with the findings of S14.

If we once again consider the simulations of Springel, Di Matteo & Hernquist (2005), this time without any feedback from black holes, they suggest that if even a small fraction of gas is not consumed in the starburst following a merger (either because the mass ratio is not large enough to cause this or from the lack of strong black hole activity) the remanent can sustain star formation for extended periods of Gyrs. The remnants from these simulations take ~ 5.5 Gyr to reach red optical colours of $u-r \sim 2.1$. We can see from our Figure 6 that models with intermediate quenching timescales of $1.0 \lesssim \tau\ [\mathrm{Gyr}] \lesssim 2.0$ take approximately $2.5 - 5.5$ Gyr to reach these red colours.

We speculate that the intermediate quenching timescales are caused by gas rich major mergers, major mergers without black hole feedback and predominantly from minor mergers. This is supported by the findings of Lotz et al. (2008) who find that the timescales for equal mass gas rich mergers with large initial separations range from $\sim 1.1 - 1.9$ Gyr and of Lotz et al. (2011), who find in further simulations, that as the baryonic gas fraction in a merger with mass ratio's of 1:1-1:4 increases, so does the timescale of the merger from ~ 0.2 Gyr (with little gas, as above for major mergers causing rapid quenching timescales) upto ~ 1.5 Gyr (with large gas fractions).

The simulations in Lotz et al. (2008) also show that the remnants of these equal mass gas rich disc mergers (wet disc mergers) are observable for $\gtrsim 1$ Gyr post merger and appear "disc-like and dusty", which is consistent with an *early-type spiral morphology*. Such galaxies are often observed to have spiral features with a dominant bulge, suggesting that such galaxies will divide the vote fractions of the GZ2 users producing $p_s \sim p_d \sim 0.5$. We believe this is why the intermediate quenching timescales are therefore the dominant features for both smooth and disc galaxies in Figures 7, 8 and 9 when these intermediate galaxies with p_s and $p_d < 0.8$ are included in the determination of the SFH parameters.

Other simulations such as Robertson et al. (2006) and Barnes (2002) support these conclusions that both gas rich major mergers and minor mergers can produce disc-like remnants. Observationally, Darg et al. (2010) showed an increase in the spiral to elliptical ratio for merging galaxies ($0.005 < z < 0.1$) by a factor of two to the general population. They attribute this to the timescales by which mergers with spirals are observable are much longer than those with elliptical galaxies, confirming once again our hypothesis about these intermediate quenching timescales. Similarly, Casteels et al. (2013) observe that galaxies ($0.01 < z < 0.09$) interacting often retain their spiral structures and that a spiral galaxy which has been classified as having 'loose winding arms' by the GZ2 users are often entering the early stages of mergers and interactions.

Whereas the disc galaxies still show a preference for slow quenching timescales across the three populations, as well as these intermediate ones, the smooth galaxies only favour these intermediate quench timescales. We find that $\sim 49\%$ of the likelihood for smooth galaxies arises due to intermediate quenching timescales; this is agreement with work done by Kaviraj (2014) who by studying SDSS photometry ($z < 0.07$), state that half of the star formation in early-type galaxies is driven by minor mergers (therefore exhausting available gas for star formation and consequently causing a gradual decline in the star formation rate). This supports earlier work by Kaviraj et al. (2011) who, using multi wavelength photometry of galaxies in COSMOS (Scoville et al. 2007), found that 70% of early-type galaxies ($0.5 < z < 0.7$) appear morphologically disturbed, suggesting either a minor or major merger in their history.

The resultant intermediate quenching timescales come from the presence of one interaction mechanism occurring, i.e. rather than for the very rapid quenching which sees a major merger combined with AGN feedback to lower the SFR over a short period of time. Therefore any external event which can cause either a burst of star formation (depleting the gas available) or directly strip a galaxy of its gas, (for example galaxy harassment, interactions, ram pressure stripping and interactions internal to clusters); would fall into the *intermediate quenching* category. Considering the majority of galaxies reside in clusters where such interactions are common, it is not surprising that the majority of our galaxies are considered to be intermediate in morphology (see Table 1).

5.3 Slow Quenching Timescales

Although intermediate quenching is the dominant mechanism across both morphological types, it cannot completely account for the quenching of disc galaxies. The preference for slow quenching timescales at early times is dominant for disc galaxies in the red sequence (and consequently traced by the green valley, see Section 8) results in galaxies with masses at the current epoch of $\log M_* \sim 11.3[M_\odot yr^{-1}]$. S14 concluded that slow quenching timescales were the most dominant mechanism for disc galaxies, however we show that intermediate quenching timescales are equally dominant.

Bamford et al. (2009) who, using GZ1 vote fractions of galaxies in the SDSS, found a significant fraction of high stellar mass red spiral galaxies in the field. This suggests that since these galaxies are mostly found in the field, where they will be isolated from the effects of interactions from other galaxies, the slow quenching mechanisms present in their preferred star formation histories must be due to secular processes; mechanisms internal to the galaxy, in the absence of sudden accretion or merger events (Kormendy & Kennicutt 2004; Sheth et al. 2012). Bar formation in a disc galaxy is such a mechanism, whereby gas is funnelled to the centre of the galaxy by the bar over long timescales where is used for star formation (consequently forming a 'pseudo-bulge'; see Kormendy et al. 2010; Simmons et al. 2013).

There is a distinct lack of high likelihood for smooth-like galaxies to undergo such slow quenching timescales; suggesting that the evolution (or indeed creation) of smooth-like galaxies is dominated by processes external to the galaxy. If we believe that these slow quenching timescales are due to secular evolution processes, this is to be expected since these processes do not change the disc dominated nature of a galaxy.

5.4 Future Work

Due to the flexibility of our model we believe that the *StarfPy* module will have a significant number of future applications, including the investigation of various different SFHs (e.g. constant SFR and starbursts). Considering the number of magnitude bands available across the SDSS, further analysis will also be possible with a larger set of optical and NUV colours, providing further constraints. If we consider that the average redshift of the GZ2 sample is z 0.076, it would also be of interest to see what this analysis would find when considering galaxies at higher redshift (e.g. out to $z \sim 1$ with Hubble Space Telescope photometry).

In particular, with further use of the robust, detailed GZ2 classifications, we believe that our module will be able to distinguish if there is any statistical difference in the star formation histories of barred vs. non-barred galaxies. This will require a simple swap of p_s and p_d with p_{bar} and p_{nobar} from the available GZ2 vote fractions. We believe that this will aid in the discussion of whether bars act to quench star formation (by funnelling gas into the galaxy centre) or promote star formation (by causing an increase in gas density as it travels through the disc) both sides of which have been fiercely argued (Masters et al. 2011, 2012; Sheth et al. 2005; Ellison et al. 2011).

Further application of the *StarfPy* code could be to investigate the parameters for currently merging/interacting pairs to those galaxies classified as merger remnants from their degree of disturbance. This will allow a direct comparison of the impact of a merger on the star formation rate of a galaxy by comparing the before and after scenario's.

It also thought that depending on the initial conditions of a galaxy merger this can either produce a slow or fast rotator elliptical galaxy. Since slow rotators are on average more massive objects that they may result from major mergers (dry) on the red sequence (Emsellem et al. 2011) , whereas fast rotators are obtained in simulations from gas rich (wet) mergers and can form more disc-like objects (Emsellem et al. 2007). By using a sample of fast and slow rotators as input galaxies we may even be able to detect a difference in the star formation histories of wet and dry mergers and in turn how these two separate populations of elliptical galaxies arose.

One of the key elements of an overarching theory of galaxy evolution is to explain how field and cluster galaxies evolve in comparison to each other. The projected neighbour density, Σ, from Baldry et al. (2006) can be used as to weight the likelihoods for cluster and field galaxies (instead of the vote fractions from GZ2 for p_s and p_d) to determine if there is a measurable statistical difference in their star formation histories.

6 CONCLUSION

We have used morphological classifications from the Galaxy Zoo 2 project to determine the morphological dependant star formation histories of galaxies through a Bayesian analysis of an exponentially declining star formation rate model of quenching. We determined the most likely parameters for the quenching time, t_q and quenching timescale τ in this model for galaxies across the blue cloud, green valley and red sequence to trace galactic evolution across the colour-magnitude diagram. In agreement with Schawinski et al. (2014) we find that the green valley is indeed a transitional population for all morphological types, however this transition proceeds slowly for the majority of disc-like galaxies and may rarely occur very rapidly for smooth-like galaxies. However, in disagreement with Schawinski et al. (2014) it is the intermediate quenching timescales which are the most dominant mechanism. Our main findings are as follows:

(i) There is a clear correlation between t_{quench} and τ. At earlier times, the quenching timescale is longer, whereas at more recent times, the quenching timescale is shorter on average suggesting an environmental quenching dependance with cosmic time

(ii) The red sequence galaxies, regardless of morphology are found to have parameter likelihoods at very similar quenching timescales to the green valley galaxies, but occurring at earlier quenching times. Therefore the quenching mechanisms currently occurring in the green valley were active in creating the red sequence at earlier times. The majority of the red sequence is quenched prior to $t \sim 6$ Gyr ($z \sim 1$) in agreement with previous studies.

(iii) The mot likely SFH parameters of both smooth- and disc-like blue cloud galaxies appear very similar suggesting galaxies in the blue cloud are similar regardless of morphology, since they are all predominantly star forming. They way these galaxies differ must therefore be in the mechanisms and triggers by which they have formed their stars having no effect on their observed colours, but a discernible effect on their morphology.

(iv) A lack of likelihood is found across all morphologies and populations of the colour-magnitude diagram for rapid ($\tau < 1.0$ Gyr) quenching timescales which is most apparent for disc galaxies. Such rapid quenching timescales are detected with a much rarer occurrence for smooth galaxies. We attribute this quenching mechanism to major mergers with black hole feedback which are able to expel the remaining gas not initially exhausted in the merger induced starburst and often causes a change in morphology from disc dominated to bulge dominated. The colour-change timescales from previous simulations of such events agree with our derived rapid timescales, along with the fraction of elliptical galaxies ($\sim 4.2\%$) with this preferred likelihood.

(v) Intermediate quenching timescales ($1.0 < \tau$ [Gyr] < 2.0) are found to be the most likely quenching mechanism for both smooth- and disc-like morphologies, the timescales for which agree with observed and simulated minor merger timescales. We hypothesise such timescales can be caused by a number of external process including gas rich major mergers, mergers without black hole feedback, galaxy harassment, interactions and ram pressure stripping. The timescales and observed morphologies from previous studies agree with our findings, including that this is the dominant

mechanisms for intermediate galaxies such as early-type spiral galaxies with spiral features but a dominant bulge which will split the GZ2 vote fractions.

(vi) Slow quenching timescales are only observed to have high likelihoods in the disc populations across the colour-magnitude diagrams, particularly in the red sequence. Such red disc galaxies are often found in the field, therefore we hypothesise that such slow quenching timescales are caused by secular evolution processes internal to the galaxy. This verifies why we do not detect a high likelihood for these slow quenching mechanisms for typical smooth galaxies as secular evolution is not capable of changing the disc dominated nature of a galaxy.

(vii) Due to the flexibility of our model we believe that the *StarfPy* module compiled for this investigation will have a significant number of future applications, including the different star formation histories of barred vs non-barred galaxies, merging vs merger remnants, fast vs slow rotating elliptical galaxies and cluster vs field galaxies.

There is not one specific route to each location of the colour-magnitude diagram, due to the complex interplay between the SFH parameters, however the morphology of a galaxy can reveal the previous possible steps to reach it's current location. If a galaxy is a late-type at the current epoch, independent of where it is on the colour-magnitude diagram) then it cannot have undergone rapid quenching and consequently any mechanism that drives this, such as a major merger. Conversely for a galaxy to be early-type at the current epoch, independent of where it is on the colour-magnitude diagram then it cannot have undergone slow quenching and consequently any mechanism that drives this, such as secular evolution.

ACKNOWLEDGEMENTS

The authors would like to thank D. Forman-Mackey and P. Marshal for extremely useful Bayesian statistics discussions and J. Binney for an interesting discussion on the nature of quenching and feedback in disc galaxies.

RS acknowledges funding from the Science and Technology Facilities Council Grant Code ST/K502236/1.

Based on observations made with the NASA Galaxy Evolution Explorer. GALEX is operated for NASA by the California Institute of Technology under NASA contract NAS5-98034

Funding for the SDSS and SDSS-II has been provided by the Alfred P. Sloan Foundation, the Participating Institutions, the National Science Foundation, the U.S. Department of Energy, the National Aeronautics and Space Administration, the Japanese Monbukagakusho, the Max Planck Society, and the Higher Education Funding Council for England. The SDSS Web Site is http://www.sdss.org/. The SDSS is managed by the Astrophysical Research Consortium for the Participating Institutions. The Participating Institutions are the American Museum of Natural History, Astrophysical Institute Potsdam, University of Basel, University of Cambridge, Case Western Reserve University, University of Chicago, Drexel University, Fermilab, the Institute for Advanced Study, the Japan Participation Group, Johns Hopkins University, the Joint Institute for Nuclear Astrophysics, the Kavli Institute for Particle Astrophysics and Cosmology, the Korean Scientist Group, the Chinese Academy of Sciences (LAMOST), Los Alamos National Laboratory, the Max-Planck-Institute for Astronomy (MPIA), the Max-Planck-Institute for Astrophysics (MPA), New Mexico State University, Ohio State University, University of Pittsburgh, University of Portsmouth, Princeton University, the United States Naval Observatory, and the University of Washington.

This publication made extensive use of the Tool for Operations on Catalogues And Tables (TOPCAT; **??**) which can be found at `http://starlink.ac.uk/topcat/`. Ages were calculated from the observed redshifts using the *cosmolopy* package provided in the Python module *astroPy*[3]; Robitaille et al. 2013). This research has also made use of NASA's ADS service and Cornell's ArXiv.

REFERENCES

Aihara, H. et al., 2011, ApJSS, 193, 29
Arnouts, S. et al., 2007, A&A, 476, 137
Baldry, I. K. et al., 2004, ApJ, 600, 681
Baldry, I. K. et al., 2006, MNRAS, 373, 469
Ball, N. M., Loveday, J. & Brunner, R. J., 2008, MNRAS, 383, 907
Bamford, S. P. et al., 2009, MNRAS, 393, 1324
Barnes, J. E. & Hernquist, L., 1996, ApJ, 471, 115
Barnes, J. E., 2002, MNRAS, 333, 481
Bell, E. F. et al., 2004, ApJ, 608, 752
Bell, E. F. et al., 2006, ApJ, 652, 270
Bell, E. F. et al., 2007, ApJ, 663, 834
Béthermin, M. et al., 2012, ApJ, 757, L23
Blanton, M. R. et al., 2005, AJ, 129, 2562
Blanton, M. R. & Roweis, S., 2007, AJ, 133, 734
Brammer, G. B. et al., 2009, ApJ, 706, 173
Brinchmann, J. et al., 2004, MNRAS, 351, 1151
Bruzual, G. & Charlot, S., 2003, MNRAS, 344, 1000
Bundy, K. et al., 2007, ApJL, 655, L5
Bundy, K. et al., 2009, ApJ, 697, 1369
Bundy, K. et al., 2010, ApJ, 719, 1969
Cardelli, J. A. et al., 1989, ApJ, 345, 245
Casteels, K. et al., 2013, MNRAS, 429, 1051
Chabrier, G., 2003, PASP, 115, 763
Chen, X. Y. et al., 2010, A&A, 515, 101
Conroy, C., Gunn, J. E. & White, M. 2009, ApJ, 699, 486
Darg, D. et al., 2010a, MNRAS, 401, 1552
Ellison, S. L. et al., 2001, MNRAS, 416, 2182
Emsellem, E. et al., 2007, IAU Symposium 235
Emsellem, E, et al., 2011, MNRAS, 414, 888
Eminian, C. et al., 2008, MNRAS, 384, 930
Faber, S. M. et al., 2007, ApJ, 665, 265
Falomo, R. et al., 2008, ApJ, 673, 694
Falkenberg, M. A. et al., 2009, MNRAS, 397, 1954
Foreman-Mackey, D., Hogg, D. W., Lang, D., Goodman, J., 2013, PASP, 125, 306
Genel, S. et al., 2008, ApJ, 688, 789
Goodman, J. & Weare, J., 2010, CAMCS, 5, 65
Gonçalves, T. S. et al., 2012, ApJ, 759, 67

[3] `http://www.astropy.org/`

González, V. et al., 2010, ApJ, 713, 115
Heinis, S. et al., 2014, MNRAS, 437, 1268
Hopkins, A. M., 2004, ApJ, 615, 209
Im, M. et al., 2002, ApJ, 571, 136
Jarosik, N. et al., 2011, ApJSS, 192, 18
Kauffman, G. et al., 2003, MNRAS, 341, 33
Kaviraj, S. et al. 2011, MNRAS, 411, 2148
Kaviraj, S., 2014, MNRAS, 440, 2944
Kormendy, J. & Kennicutt, R. J., 2004, ARA&A, 42, 603
Kormendy, J. et al., 2010, ApJ, 723, 54
Kriek, M. et al., 2010, ApJL, 722, L64
Lintott, C. J. et al., 2011, MNRAS, 410, 166
Lotz, J. et al., 2008, MNRAS, 391, 1137
Lotz, J. et al., 2011, MNRAS, 742, 103
MacKay, D. J. C., 2003, *Information Theory, Inference and Learning Algorithms*, Cambridge University Press, ISBN 978-0-521-64298-9
Marasco, A., Fraternali, F. & Binney, J. J., 2012, MNRAS, 419, 1107
Maraston, C., 2005, MNRAS, 362, 799
Marigo, P. & Girardi, L. 2007, A&A, 469, 239
Martin, D. C. et al., 2005, ApJ, 619, L1
Martin, D. C. et al., 2007, ApJS, 173, 342
Masters, K. L. et al., 2010, MNRAS, 405, 783
Masters, K. L. et al., 2011, MNRAS, 411, 2026
Masters, K. L. et al., 2012, MNRAS, 424, 2180
Melbourne, J. et al., 2012, ApJ, 748, 47
Mendez, A. J. et al., 2011, ApJ, 736, 110
Miller, N. A., Rose, J. A. & Cecil, G. 2011, ApJL, 727, L15
Nair, P. B. & Abraham, R. G. 2010, ApJSS, 186, 427
Noeske, K. G. et al., 2007, ApJ, 660, L43
Oh, K. et al., 2011, ApJS, 195, 13
Padmanabhan, N. et al., 2008, ApJ, 674, 1217
Peng, Y. et al., 2010, ApJ, 721, 193
Robertson, B. et al., 2006, ApJ, 645, 986
Robitaille, T. P. et al., 2013, A&A, 558, A33
Salim, S. et al., 2007, ApJSS, 173, 267
Schawinski, et al., 2007, MNRAS, 382, 1415
Schawinski, K. et al., 2009, MNRAS, 396, 818
Schawinski, K. et al., 2014 (arXiv: 1402.4814)
Schiminovich, D. et al., 2007, ApJS, 173, 315
Scoville, N. et al., 2007, ApJSS, 172, 1
Sheth, K. et al., 2005, ApJ, 632, 217
Sheth, K. et al., 2012, ApJ, 758, 136
Simmons, B. D. et al., 2013, MNRAS, 429, 2199
Sivia, D. S., 1996, *Data Analysis: A Bayesian Tutorial*, Oxford University Press, ISBN 0-19-851889-7
Skibba, R. A. et al., 2009, MNRAS, 399, 966
Springel, V., Di Matteo, T. & Hernquist, L., 2005, ApJ, 620, L79
Soklakov, A. N., 2002, (arXiv:math-ph/0009007)
Taylor, M. B., 2005, ASP Conference Series, 347
Tojeiro, R. et al., 2013, MNRAS, 432, 359
Willett, K. et al., 2014, MNRAS, 435, 2835
Willmer, C. N. A. et al., 2006, ApJ, 647, 853
Wyder, T. K. et al., 2007, ApJS, 173, 293
York, D. G. et al., 2000, AJ, 120, 1579